Incorporating sulfur reactions and interactions with iron and phosphorus into a general plant-wide model

Hélène Hauduc, Tanush Wadhawan, Bruce Johnson, Charles Bott, Matthew Ward and Imre Takács

ABSTRACT

Sulfur causes many adverse effects in wastewater treatment and sewer collection systems, such as corrosion, odours, increased oxygen demand, and precipitate formation. Several of these are often controlled by chemical addition, which will impact the subsequent wastewater treatment processes. Furthermore, the iron reactions, resulting from coagulant addition for chemical P removal, interact with the sulfur cycle, particularly in the digester with precipitate formation and phosphorus release. Despite its importance, there is no integrated sulfur and iron model for whole plant process optimization/design that could be readily used in practice. After a detailed literature review of chemical and biokinetic sulfur and iron reactions, a plant-wide model is upgraded with relevant reactions to predict the sulfur cycle and iron cycle in sewer collection systems, wastewater and sludge treatment. The developed model is applied on different case studies.

Key words | anaerobic digestion, iron, sewer, sulfur, wastewater treatment, whole plant modelling

Hélène Hauduc (corresponding author)
Tanush Wadhawan
Imre Takács
Dynamita SARL,
7 LD Eoupe,
Nyons,
France
E-mail: helene@dynamita.com

Bruce Johnson
Jacobs,
Denver, CO,
USA

Charles Bott
HRSD,
Norfolk, VA,
USA

Matthew Ward
Jacobs,
Austin, TX,
USA

INTRODUCTION

Sulfur (S) comes right after the five key elements (C, O, H, N, P) by weight in activated sludge. Sulfur amounts to about 1% of dry weight of microorganisms; it is essential for life and is involved in a complex network of biological and chemical reactions. In its various forms, it can exert oxygen demand, can be used as electron acceptor or donor, can produce inert precipitates thus increasing sludge production, and can bind iron in the digester and lead to additional P release (Batstone *et al.* 2015). Furthermore, gaseous hydrogen sulfide is known to result in sulfide oxidation which results in corrosive sulfuric acid on concrete sewer surfaces exposed to air (Parker 1945). Many of the organic and inorganic forms of sulfur cause odour nuisances (WERF 2007), and corrosion in digester gas co-generation systems. Sulfur in wastewater collection systems is often handled through chemical additions (e.g. nitrate, H_2O_2, NaOCl, iron, $Mg(OH)_2$, NaOH, $Ca(OH)_2$) (Hvitved-Jacobsen *et al.* 2013), which will impact the subsequent wastewater treatment processes. Furthermore the iron reactions, resulting from addition for chemical P removal and digester gas H_2S control, interact with the

sulfur cycle, particularly in the digester with precipitate formation (Roussel & Carliell-Marquet 2016).

Despite its large importance, there was no integrated sulfur and iron model for whole plant process optimization/design that could be used in practice at the beginning of this study. However, there is a large amount of literature describing the individual biological or chemical reactions and redox transformations (Batstone *et al.* 2015). What is missing is integration with existing whole plant models and calibration to real world data and scenarios.

The objective of this work is to upgrade a whole plant model with a reliable description of sulfur and iron precipitation, volatilization, oxidation and reduction processes. The challenge in such complex systems is to keep the global model as simple as possible (i.e. limiting the number of biomasses and kinetic processes), and to develop a model able to predict the sulfur and iron cycle in sewer systems (aerobic/anoxic/anaerobic conditions with low biomass concentration), in wastewater treatment processes (aerobic/anoxic/anaerobic) and in solids treatment processes (anaerobic digesters). The sulfur and iron

reactions implemented in the model are based on a detailed literature review.

SULFUR AND IRON BIOLOGY AND CHEMISTRY: LITERATURE REVIEW AND MODEL EXTENSION

The plant-wide model proposed in this study is a 'standard supermodel' (Grau *et al.* 2009), all processes that can occur in the collection system, in the mainstream and in the sludge line being in a single model. The main advantages of a supermodel are the absence of interfaces to connect two standard models (as would be necessary with an 'interfaces' approach using, for example, activated sludge model (ASM)-type and anaerobic digestion model (ADM)-type models) and the absence of required knowledge on the biochemical processes that might occur to adapt the model to the plant under study ('tailored supermodel'). However, the 'standard supermodel' has a higher computational cost, as all equations of the model are solved in each process unit of the configuration, which causes a minimal overload using a simulation platform with efficient algorithms.

A plant-wide model of phosphorus transformation including interlinks with sulfur and iron cycles has been proposed by Solon *et al.* (2017). This plant-wide model is based on ASM2d model for the mainstream and on ADM1 for the sludge line. Interfaces are required between the biokinetic models and the physico-chemical models. The physico-chemical model and the biochemical processes considered

by Solon *et al.* (2017) are overall similar to those proposed in this study for a conventional water resource and recovery plant. However, some iron and sulfur reduction processes are not implemented in this extended ASM2d model, which could limit the applicability of the model in the case of low oxidation/reduction potential (ORP) zones (e.g. sections of collection systems, and sidestream enhanced biological phosphorus removal).

Whole plant model background

The base model is a plant-wide model (Dynamita 2016) considering typical biological and physio-chemical reactions of activated sludge and anaerobic digestion. It considers different organisms groups: (i) heterotrophs (biochemical oxygen demand (BOD) removal and denitrification in one or two steps); (ii) methanol utilizers (BOD removal under anoxic conditions); (iii) nitrifiers (one- or two-step nitrification); (iv) anammox organisms; (v) phosphate accumulating organisms, considering their behaviour under low ORP conditions and competition with glycogen accumulating organisms (Varga *et al.* 2018); and (vi) acidoclastic (AMETO) and hydrogenotrophic methanogens (HMETO).

The physio-chemical model considers: (i) chemical phosphorus removal (iron dosing, based on surface complexation model concepts (Hauduc *et al.* 2015)); (ii) precipitation reactions (forming amorphous calcium phosphate, calcium carbonate, struvite, vivianite); (iii) chemical equilibrium (ionic speciation) for pH calculation; and (iv) gas transfer.
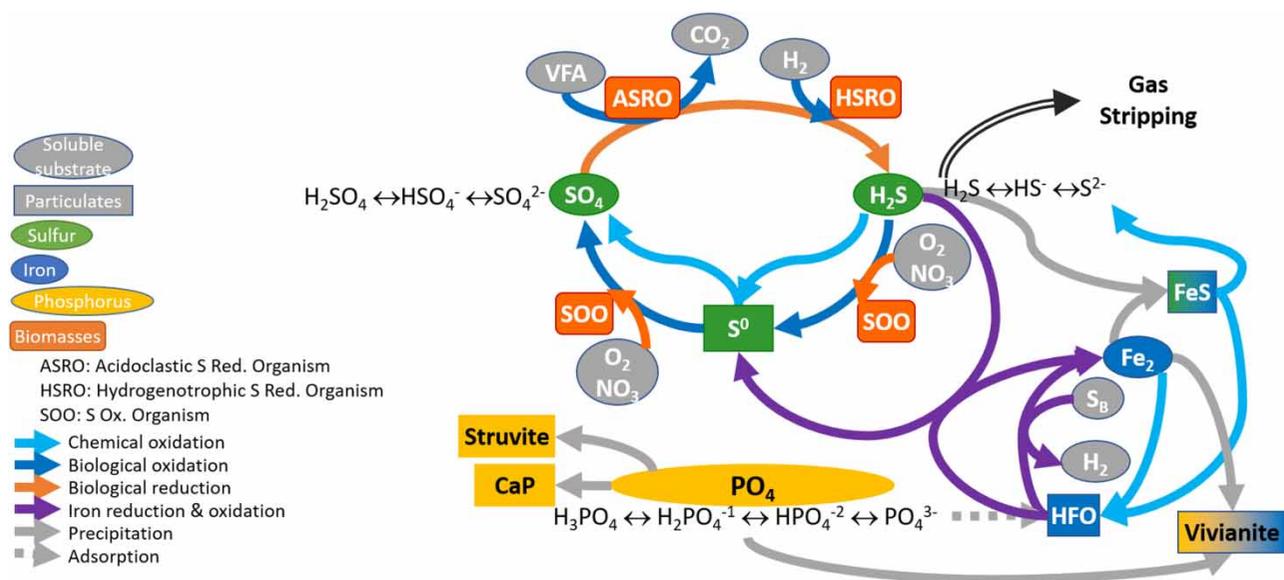

Figure 1 │ Phosphorus, sulfur and iron cycles interaction implemented in the plant-wide model.

Biology and chemistry were extended with required components, species and reactions in accordance with the following literature review. Figure 1 synthesizes the sulfur cycle implemented in Sumo© models (Dynamita 2018) and the interactions with phosphorus and iron cycles.

General sulfur and iron model

The sulfur model included in Sumo includes three oxidation states of sulfur: sulfate (SO_4^{-2}) as S_{SO4}, elemental sulfur (S^0) as X_S, and sulfide (S^-) as S_{H2S}.

Considering iron, two oxidation states are included in the model. Hydrous ferric oxides (HFO) species are already included in the base model for the chemical phosphorus treatment. These state variables ($X_{HFO,H}$, $X_{HFO,L}$, $X_{HFO,old}$, $X_{HFO,H,P}$, $X_{HFO,L,P}$, $X_{HFO,H,P,old}$ and $X_{HFO,L,P,old}$ depend on the floc size and P-bound status) are considered to be the only ferric (Fe^{3+}) species in the model, as ferric iron is only minimally soluble in water (Hauduc *et al.* 2015). X_{HFO} is a calculated variable being the sum of the seven HFO state variables. For the ferrous iron (Fe^{2+}), a new state variable is included in the model as S_{Fe2}, and ferrous oxides are not considered.

These states are considered to interact with other wastewater components as described below.

FeS precipitation and iron interaction

Reduction of Fe^{3+}, sulfide as electron donor

A chemical reduction of Fe^{3+} by sulfide occurs under reducing conditions. In this reaction, sulfide is oxidized into colloidal elemental sulfur which precipitates (Nielsen *et al.* 2005; Firer *et al.* 2008):

$$2Fe^{3+} + HS^- \rightarrow 2Fe^{2+} + S^0 + H^+$$
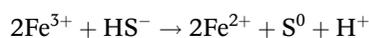
Implementation in the whole plant model. Elemental sulfur has been added as a particulate state variable (X_S), as elemental sulfur has a low solubility and flocculates easily. The hydrous ferric oxides (X_{HFO}) are reduced by H_2S in a single process into ferrous iron (S_{Fe2}) and elemental sulfur (X_S) with adequate stoichiometric coefficient to balance the redox reaction and a first order rate with respect to the X_{HFO} concentration.

### Reduction of Fe^{3+}, organic matter as electron donor

HFO are reduced in digesters into soluble Fe^{2+} which precipitates into iron sulfide (FeS), and release bound phosphates (Ge *et al.* 2013), which can further precipitate into vivianite ($Fe_3(PO_4)_2,8H_2O$) (Cheng *et al.* 2015). This biological process is performed by Fe^{3+}-reducing bacteria, using organic matter as electron donors (Lovley & Phillips 1988).

Implementation in the whole plant model. To keep the model simple, the small amount of iron-reducing biomass production is not introduced in the model. The soluble biodegradable substrate (S_B) and volatile fatty acids (S_{VFA}) are considered as electron donor, and a first order kinetic rate expression with respect to the X_{HFO} concentration is used.

FeS precipitation

Fe^{2+} precipitates with sulfide into FeS (Nielsen *et al.* 2005; Firer *et al.* 2008):

$$Fe^{2+} + HS^- \rightarrow FeS + H^+$$
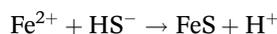
Implementation in the whole plant model. The acid-base reactions of the sulfate and sulfide species are added in the pH model for speciation (equilibrium model). The precipitation is modelled following the Koutsoukos *et al.* (1980) kinetic expression with a solubility product $K_{sp,FeS} = 3.7*10^{-19}$ (Nielsen *et al.* 2005).

Oxidation of Fe^{2+}

According to Gutierrez *et al.* (2010), the precipitated FeS is re-oxidized into ferric oxides and sulfate in an aerobic zone.

Implementation in the whole plant model. Both oxidation of ferrous iron (S_{Fe2}) and precipitated iron sulfide (X_{FeS}) are considered in the model with oxygen as electron acceptor with adequate stoichiometric coefficients to balance the redox reaction and a first order rate with respect to the S_{Fe2} and X_{FeS} concentrations respectively.

Reduction of sulfate

The biological sulfate reduction is the main process step in sulfur biotreatment, often combined with a chemical step or a metal precipitation step (Hao *et al.* 2014). The biological sulfate reduction is performed by sulfate-reducing organisms (SRO), which can use either hydrogen or organic compounds as electron donor. These bacteria are directly in competition with hydrogenotrophic and acetoclastic methanogens respectively in anaerobic bioprocesses (Kalyuzhnyi & Fedorovich 1998; Chou *et al.* 2008; Hao *et al.* 2014) and

in sewer sediments (Liu *et al.* 2016). Models for sewer systems usually neglect the biomass growth whereas models for anaerobic digestion always consider it. These models consider different kinds of substrates. Knobel & Lewis (2002) consider five substrates, and Liu *et al.* (2015) and Fedorovich *et al.* (2003) consider four substrates, whereas Batstone (2006) suggests considering only hydrogenotrophic sulfate reducer bacteria if sulfur to chemical oxygen demand (COD) ratio is below 0.1 mg S/mg COD. The best compromise seems to be the model from Barrera *et al.* (2015) and Poinapen & Ekama (2010) who consider H_2, acetate and propionate as substrates. The WATS (wastewater aerobic–anaerobic transformations in sewers) model for sewer processes (Hvitved-Jacobsen *et al.* 2013) considers only soluble substrate for sulfate reduction biological processes.

Implementation in the whole plant model. Considering the actual structure of the extended version of Sumo model, S_{VFA} and S_{H2} have been chosen as substrate for SRO, resulting in competition with the AMETO and HMETO, which would be similar to what is suggested by Barrera *et al.* (2015) and in accordance with Kalyuzhnyi & Fedorovich (1998). Similarly to the methanogenesis implementation, two biomasses are introduced: acidoclastic sulfate-reducing organisms and hydrogenotrophic sulfate-reducing organisms. This leads to four additional processes to consider growth and decay of both biomasses. Stoichiometric and kinetic values from Barrera *et al.* (2015) are used. The produced sulfide is inhibitory (Utgikar *et al.* 2002). It has been considered in the kinetic rate expression through Haldane functions when sulfide is a reactant of the process, otherwise through Monod limitation function term.

Oxidation of sulfide

Biological oxidation

The biological oxidation of sulfide into sulfate is performed through intermediate species. The oxidation may use either oxygen, nitrite or nitrate as electron acceptor. In the literature, the biological oxidation of sulfide is mainly modelled in one or two steps, S^0 being the intermediate. The oxidation of elemental sulfur to sulfate is the limiting step (Buisman *et al.* 1991; Tichy *et al.* 1998; Jiang *et al.* 2009). According to several authors, when sulfide is oxidized in a digester at limiting oxygen levels, it is converted to elemental sulfur which precipitates, making it less available for further biological reduction (Jenicek *et al.* 2008; Díaz & Fdz-Polanco 2012).

Implementation in the whole plant model. A sulfur oxidizing organism (X_{SOO}) has been introduced in the model with four oxidation processes to consider the two steps of sulfide oxidation and two possible oxidants (O_2 and NO_3). The parameter values from Mannucci *et al.* (2012) are used as first estimation.

Chemical oxidation

At high SOO activity, chemical oxidation is negligible (Luther *et al.* 2011) but must be considered in the case of sewer processes with lower biomass concentration, as the oxygen consumption for sulfide oxidation counts significantly in the oxygen uptake rate (OUR) (Nielsen *et al.* 2003). The literature reports kinetic laws with different orders and a wide range of oxidation rate parameters; however, the rate of the two steps of oxidation are not determined independently (Buisman *et al.* 1990; Nielsen *et al.* 2003; Luther *et al.* 2011; Hvitved-Jacobsen *et al.* 2013; Klok *et al.* 2013).

Implementation in the whole plant model. Two processes for oxidation of S_{H2S} by oxygen in two steps ($S_{H2S} \rightarrow X_S \rightarrow S_{SO4}$) is added. All the oxidation intermediates are considered through the elemental sulfur state variable (X_S), whereas the second oxidation step ($X_S \rightarrow S_{SO4}$) is much slower (Nielsen *et al.* 2003). To simplify the model, first order reactions with respect to sulfide and to elemental sulfur have been implemented for both steps of the oxidation process.

The full Gujer matrix of the model is available as supplementary material (http://www.dynamita.com/public/models/Sumo2S.xlsm).

RESULTS

The whole plant model behaviour is evaluated for collection system, mainstream and sludge line. All the results presented are obtained using a single set of parameters.

Sewer pipe example

A force main sewer pipe with no gas phase has been modelled by 10 segments of 1.2 h hydraulic retention time (HRT) each, so a total HRT of 12 h over the pipe. The sewer biofilm is not modelled here as it will be part of a further process unit model development. Only reactions occurring in the bulk are considered.

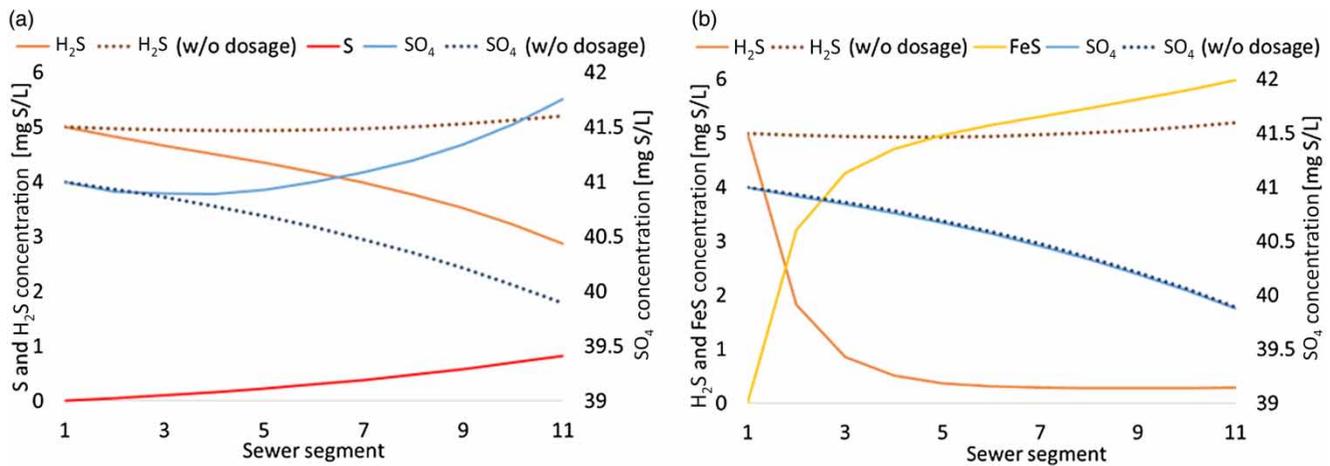The simulation without any dosage shows a slight reduction of sulfate along the sewer pipe (dotted lines on

Figure 2 │ Sulfur component concentrations in the sewer pipe with (a) nitrate dosage (solid lines) and (b) iron dosage (solid lines) and without dosage (dotted lines).

Figure 2) due to sulfate-reducing bacteria activity, in the absence of electron acceptors. With nitrate dosage, sulfide is oxidized into elemental sulfur (X_S) that precipitates, then into sulfate (Figure 2(a)). The accumulation of elemental sulfur confirms that in the model the oxidation of elemental sulfur to sulfate is the limiting step as stated by many authors (Buisman *et al.* 1991; Tichy *et al.* 1998; Jiang *et al.* 2009). With Fe^{2+} dosage, Fe^{2+} strongly binds sulfide into FeS, which precipitates (Figure 2(b)).

The produced compounds in each case (X_S and X_{FeS} respectively), will be either captured with primary treatments or oxidized in aerated processes of the downstream wastewater treatment plant.

Mainstream modelling

Concerning the wastewater treatment, an idealized UCT (University of Cape Town) plant was simulated. Results show sulfide oxidation into sulfate in anoxic and aerobic tanks (Figure 3) with nitrate and oxygen respectively.

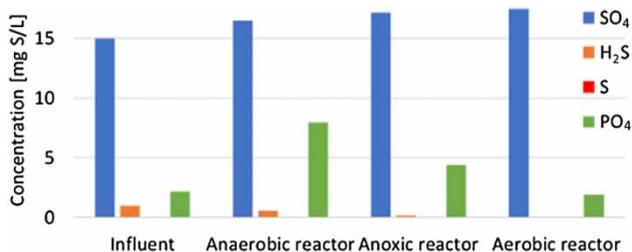The impact of sulfur on the oxygen demand has been investigated on this configuration. A first run with the base model that does not include the sulfur implementation shows an OUR of 34.7 mg O_2/(L·h) for a dissolved oxygen controlled at 2 mg/L in the aerobic tank. Then, influent total sulfur concentrations from 10 mg S/L to 100 mg S/L with a sulfide fraction of 5% (0–5 mg S-H_2S/L), 10% (0–10 mg S-H_2S/L) and 20% (0–20 mg S-H_2S/L) are simulated with the new model. The influent sulfide fraction depends on the length and characteristics of the sewer network.

Figure 4 shows the impact of the influent sulfur concentration and sulfide fraction on OUR. The shape of the curve is driven by the biological oxidation of elemental sulfur to sulfate by SOO biomass, which is known to be the limiting oxidation step (Mannucci *et al.* 2012). From this result, an influent concentration of 20 mg S/L causes an underestimation of OUR of around 5% for an influent sulfide fraction from 5% to 20%. For an influent concentration of 100 mg S/L, the underestimation of OUR goes from 7% (for an influent sulfide fraction of 5%) to 17% (for an influent sulfide fraction of 20%).
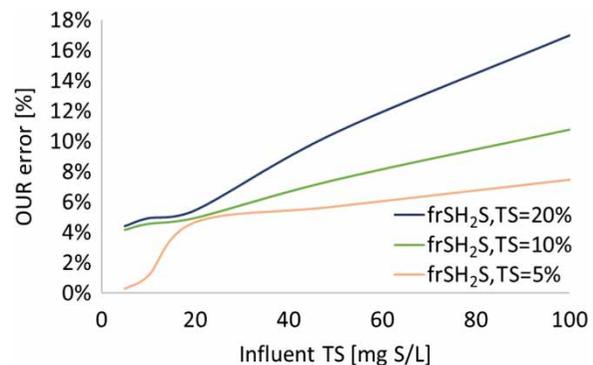

Figure 3 │ Sulfur forms through the wastewater treatment (influent total sulfur of 10 mg S/L).

Figure 4 │ Impact of influent total sulfur (TS) on OUR in the aeration tank with an influent sulfide fraction of 5%, 10% and 20% of total sulfur.

Digester modelling

A UCT plant with primary and waste sludge digestion is simulated to evaluate the impact of sulfur on the digester. A plant influent total sulfur of 20 mg/L and a S:COD ratio of 0.004 g S/g COD at the digester influent leads to a hydrogen sulfide concentration of 5,000 ppm in the biogas, which is similar to what is modelled by Flores-Alsina *et al.* (2016) for this range of S:COD ratio. The sulfate reduction and hydrogen sulfide production in the biogas are due to the biological activity of the sulfate-reducing bacteria, which can either use VFA (S_{VFA}) or dissolved hydrogen (S_{H2}) as electron acceptor in the model. They are in direct competition with methanogens, reducing the methane production from 1,289 m^3/d (model without sulfur) to 1,283 m^3/d, with respectively a methane content in the biogas of 66.1% and 64.9%.

Iron is widely used in water resource recovery facilities (WRRFs), either for phosphorus chemical treatment or to limit H_2S formation in the digester. The unintended consequence on digestion is the precipitation of iron into vivianite with phosphorus and into FeS or pyrite with sulfide. For a plant influent of 20 mg S/L, iron doses from 0 to 30 g/kg of digester dry solids are simulated to compare with Roussel & Carliell-Marquet (2016) work. Figure 5 shows the results, with first the precipitation of FeS, then of vivianite, with very close values to those of Roussel & Carliell-Marquet (2016). Figure 5 furthermore shows the decrease of hydrogen sulfide in the biogas as FeS precipitates.

The Lander Street WRRF (Boise, Idaho, USA) was experiencing problems with high hydrogen sulfide content of the biogas and struvite precipitations, resulting in increased maintenance requirements. A study was performed to evaluate the required doses of iron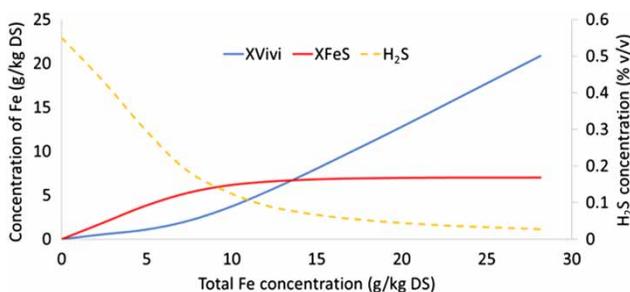 to solve these two problems, by precipitating sulfide and phosphorus. A sampling programme of 45 days around the primary digester provided good knowledge of its operation performance (Table 1). The primary digester is simulated with equivalent total solids and elemental loads of nitrogen, phosphorus, sulfur, calcium and magnesium. The model results are similar to the measured data, especially concerning gas production, and hydrogen sulfide and phosphate concentrations.

For this study, doses of 25 g $FeCl_3$/kg VSS (volatile suspended solids) and of 100 g $FeCl_3$/kg VSS were estimated by experts to control respectively hydrogen sulfide and struvite precipitation. These doses were applied in the simulation and results are shown in Table 1. With dosage for H_2S control, the model correctly predicts the reduction of hydrogen sulfide by more than 10 times (from 1,926 ppm to 141 ppm)

Figure 5 | Iron precipitates in function of iron dose and impact on H_2S concentration in the biogas.

Table 1 | Data and simulation results of Lander Street primary digester, and two scenarios of iron dose for hydrogen sulfide and struvite control

| Parameter | Data | **Model** | | |
		without iron	with iron for H_2S control	with iron for struvite control
Iron dose, g $FeCl_3$/kg VSS		0	25	100
Influent total nitrogen, kg/d	306	308		
Influent total phosphorus, kg/d	90	89		
Influent total sulfur, kg/d	23	27		
Influent Ca, kg/d	127	128		
Influent Mg, kg/d	17	17		
Influent total solids	4.0%	4.0%		
Influent VSS, % of total solids	84%	85%		
Digester total solids	1.70%	2.10%	2.15%	2.24%
Digester VSS, % of total solids	67%	66%	65%	62%
Digester pH	7.15	7.16	7.07	6.80
Alkalinity as $CaCO_3$, mg/L	4,100	3,544	2,939	1,762
Gas production, Nm^3/h	176	172	174	178
Digester gas H_2S, ppm	**2,125**	**1,926**	**141**	**4**
Digester ammonia, mg N/L	1,169	979	978	1,018
Digester phosphate, mg P/L	156	166	113	2
Struvite, mg TSS/L	**?**	**842**	**827**	**37**
Vivianite, mg TSS/L		0	578	2,488
Iron sulfide, mg TSS/L		0	146	163
Elemental sulfur, mg S/L		0	3	1
Amorphous calcium phosphate, mg TSS/L		300	186	2

VSS: volatile suspended solids; TSS: total suspended solids.
Bold text refers to parameters controlled with iron dosing.

as expected by the experts with a dose of 25 g FeCl$_3$/kg VSS, by precipitating sulfide into FeS. This process requires first the reduction of Fe^{3+} into Fe^{2+}, which is also correctly predicted. Furthermore, the 100 g FeCl$_3$/kg VSS dosage is shown to reduce drastically the struvite precipitation (from 842 mg TSS/L to 37 mg TSS/L), while increasing vivianite precipitation and decreasing phosphate concentration in the digester.

DISCUSSION

The application of the whole plant model behaviour for collection system, mainstream and sludge line enable evaluation of the new processes implemented. The modelling exercise on a sewer segment shows the potential of the model to simulate the behaviour of sulfur species and to evaluate the impact of dosing treatments in a segment of sewer system. It involves biological reduction of sulfate when no dosing is applied. The simulation of nitrate dosage shows the behaviour of chemical and biological sulfide oxidation processes and the kinetically limited oxidation of elemental sulfur. However, those simulations doe not take the biofilm in the sewer into account and thus neglect substantially the biological reactions that take place in the collection system. An adequate process unit model considering the biofilm is required as further development.

The application of the model on a typical mainstream configuration shows the impact of the sulfide oxidation on OUR and emphasizes the need to take into account sulfur reactions to appropriately model the oxygen demand depending on the influent sulfur concentrations and the length and characteristics of the sewer network. Furthermore, in the case of carbon source limitation, the sulfur-reducing organisms will be directly competing with the phosphorus accumulating organisms, reducing the biological phosphorus removal, which is not illustrated with this example.

The interconnections of phosphorus, iron and sulfur cycles are better demonstrated with the digester modelling. The role of sulfate-reducing bacteria in the production of hydrogen sulfide is shown by the model, which manages to predict the biogas quality accurately. The effect of iron dose on the biogas quality and precipitates is appropriately described, which gives confidence in the physical–chemical model. The precipitation processes are all implemented with the Koutsoukos *et al.* (1980) kinetic rate expression type, meaning that the precipitation rate depends on the distance

to the thermodynamical equilibrium of the precipitate and on a kinetic rate parameter. The competition between different precipitates for the same ions will thus depend on the thermodynamic constants and on the kinetic rate parameters that must be calibrated. Both case studies show the ability of the model to predict the sequence of precipitates: in the presence of sulfur, iron dosage will first lead to iron sulfide precipitation, then to vivianite precipitation. The vivianite precipitation will thus compete with other phosphate precipitates, and especially with struvite as illustrated in Table 1.

CONCLUSIONS

Sulfur chemistry and biology occurring in activated sludge treatment, anaerobic digestion and sewers were introduced: (i) reduced and oxidized S species within the weak acid-base chemistry framework; (ii) biological oxidation/reduction, including the S$_0$ step; (iii) chemical redox reactions (sulfur oxidizes/reduces abiotically as well); (iv) H$_2$S gas transfer; (v) Fe^{2+} and Fe^{3+} redox transformations to be able to predict S bound with Fe in the digester; and (vi) extended Fe^{2+} and Fe^{3+} chemistry (hydroxides, HFO and vivianite formation).

The model can be used to develop strategies to cope with hydrogen sulfide production and optimize iron and nitrate addition in sewers, predict vivianite build-up in digesters, calculate oxygen demand of hydrogen sulfide in anaerobic wastewaters or return liquids, and correct pH predictions as hydrogen sulfide is a weak acid and sulfate is a strong acid.

SUPPLEMENTARY MATERIAL

The full Gujer matrix and parameters of the model can be downloaded at the following link: http://www.dynamita. com/public/models/Sumo2S.xlsm.

REFERENCES

Barrera, E. L., Spanjers, H., Solon, K., Amerlinck, Y., Nopens, I. & Dewulf, J. 2015 Modeling the anaerobic digestion of cane-molasses vinasse: extension of the anaerobic digestion model no. 1 (ADM1) with sulfate reduction for a very high strength and sulfate rich wastewater. *Water Research* **71**, 42–54.

Batstone, D. J. 2006 Mathematical modelling of anaerobic reactors treating domestic wastewater: rational criteria for model use.

Reviews in Environmental Science and Bio/Technology **5** (1), 57–71.

Batstone, D. J., Puyol, D., Flores-Alsina, X. & Rodríguez, J. 2015 Mathematical modelling of anaerobic digestion processes: applications and future needs. *Rev. Environ. Sci. Biotechnol.* **14**, 595–613.

Buisman, C., Uspeert, P., Janssen, A. & Lettinga, G. 1990 Kinetics of chemical and biological sulphide oxidation in aqueous solutions. *Water Research* **24** (5), 667–671.

Buisman, C., Ijspeert, P., Hof, A., Janssen, A., Tenhagen, R. & Lettinga, G. 1991 Kinetic parameters of a mixed culture oxidizing sulfide and sulfur with oxygen. *Biotechnology and Bioengineering* **38** (8), 813–820.

Cheng, X., Chen, B., Cui, Y., Sun, D. & Wang, X. 2015 Iron(III) reduction-induced phosphate precipitation during anaerobic digestion of waste activated sludge. *Separation and Purification Technology* **143**, 6–11.

Chou, H.-H., Huang, J.-S., Chen, W.-G. & Ohara, R. 2008 Competitive reaction kinetics of sulfate-reducing bacteria and methanogenic bacteria in anaerobic filters. *Bioresource Technology* **99** (17), 8061–8067.

Díaz, I. & Fdz-Polanco, M. 2012 Robustness of the microaerobic removal of hydrogen sulfide from biogas. *Water Science and Technology* **65**, 1368–1374.

Dynamita 2016 *Sumo User Manual*.

Dynamita 2018 http://www.dynamita.com/wp-content/uploads/Sumo2S.xlsm.

Fedorovich, V., Lens, P. & Kalyuzhnyi, S. 2003 Extension of anaerobic digestion model no. 1 with processes of sulfate reduction. *Applied Biochemistry and Biotechnology* **109** (1–3), 33–46.

Firer, D., Friedler, E. & Lahav, O. 2008 Control of sulfide in sewer systems by dosage of iron salts: comparison between theoretical and experimental results, and practical implications. *Science of the Total Environment* **392** (1), 145–156.

Flores-Alsina, X., Solon, K., Kazadi Mbamba, C., Tait, S., Gernaey, K. V., Jeppsson, U. & Batstone, D. J. 2016 Modelling phosphorus (P), sulfur (S) and iron (Fe) interactions for dynamic simulations of anaerobic digestion processes. *Water Research* **95**, 370–382. https://doi.org/10.1016/j.watres.2016.03.012.

Ge, H., Zhang, L., Batstone, D. J., Keller, J. & Yuan, Z. 2013 Impact of iron salt dosage to sewers on downstream anaerobic sludge digesters: sulfide control and methane production. *Journal of Environmental Engineering* **139** (4), 594–601.

Grau, P., Copp, J., Vanrolleghem, P. A., Takács, I. & Ayesa, E. 2009 A comparative analysis of different approaches for integrated WWTP modelling. *Water Science and Technology* **59**, 141–147. https://doi.org/10.2166/wst.2009.589.

Gutierrez, O., Park, D., Sharma, K. R. & Yuan, Z. 2010 Iron salts dosage for sulfide control in sewers induces chemical phosphorus removal during wastewater treatment. *Water Research* **44** (11), 3467–3475.

Hao, T., Xiang, P., Mackey, H. R., Chi, K., Lu, H., Chui, H., van Loosdrecht, M. C. M. & Chen, G.-H. 2014 A review of

biological sulfate conversions in wastewater treatment. *Water Research* **65**, 1–21.

Hauduc, H., Takács, I., Smith, S., Szabo, A., Murthy, S., Daigger, G. T. & Spérandio, M. 2015 A dynamic physicochemical model for chemical phosphorus removal. *Water Research* **73**, 157–170.

Hvitved-Jacobsen, T., Vollertsen, J. & Nielsen, A. H. 2013 *Sewer Processes: Microbial and Chemical Process Engineering of Sewer Networks*, 2nd edn. CRC Press, Boca Raton, FL, USA.

Jenicek, P., Keclik, F., Maca, J. & Bindzar, J. 2008 Use of microaerobic conditions for the improvement of anaerobic digestion of solid wastes. *Water Science and Technology* **58**, 1491–1496.

Jiang, G., Sharma, K. R., Guisasola, A., Keller, J. & Yuan, Z. 2009 Sulfur transformation in rising main sewers receiving nitrate dosage. *Water Research* **43** (17), 4430–4440.

Kalyuzhnyi, S. V. & Fedorovich, V. V. 1998 Mathematical modelling of competition between sulphate reduction and methanogenesis in anaerobic reactors. *Bioresource Technology* **65** (3), 227–242.

Klok, J. B. M., de Graaff, M., van den Bosch, P. L. F., Boelee, N. C., Keesman, K. J. & Janssen, A. J. H. 2013 A physiologically based kinetic model for bacterial sulfide oxidation. *Water Research* **47** (2), 483–492.

Knobel, A. N. & Lewis, A. E. 2002 A mathematical model of a high sulphate wastewater anaerobic treatment system. *Water Research* **36** (1), 257–265.

Koutsoukos, P., Amjad, Z., Tomson, M. B. & Nancollas, G. H. 1980 Crystallization of calcium phosphates. A constant composition study. *Journal of the American Chemical Society* **102** (5), 1553–1557.

Liu, Y., Zhang, Y. & Ni, B.-J. 2015 Evaluating enhanced sulfate reduction and optimized volatile fatty acids (VFA) composition in anaerobic reactor by Fe (III) addition. *Environmental Science & Technology* **49** (4), 2123–2131.

Liu, Y., Tugtas, A. E., Sharma, K. R., Ni, B-J & Yuan, Z. 2016 Sulfide and methane production in sewer sediments: field survey and model evaluation. *Water Research* **89**, 142–150.

Lovley, D. & Phillips, E. 1988 Novel mode of microbial energy-metabolism – organic-carbon oxidation coupled to dissimilatory reduction of iron or manganese. *Applied and Environmental Microbiology* **54** (6), 1472–1480.

Luther, G. W., Findlay, A. J., MacDonald, D. J., Owings, S. M., Hanson, T. E., Beinart, R. A. & Girguis, P. R. 2011 Thermodynamics and kinetics of sulfide oxidation by oxygen: a look at inorganically controlled reactions and biologically mediated processes in the environment. *Frontiers in Microbiology* **2**, 62.

Mannucci, A., Munz, G., Mori, G. & Lubello, C. 2012 Biomass accumulation modelling in a highly loaded biotrickling filter for hydrogen sulphide removal. *Chemosphere* **88**, 712–717.

Nielsen, A. H., Vollertsen, J. & Hvitved-Jacobsen, T. 2003 Determination of kinetics and stoichiometry of chemical sulfide oxidation in wastewater of sewer networks. *Environmental Science & Technology* **37** (17), 3853–3858.

Nielsen, A. H., Lens, P., Vollertsen, J. & Hvitved-Jacobsen, T. 2005 Sulfide–iron interactions in domestic wastewater from a gravity sewer. *Water Research* **39** (12), 2747–2755.

Parker, C. D. 1945 The corrosion of concrete. I. The isolation of a species of bacterium associated with corrosion of concrete exposed to atmospheres containing hydrogen sulphide. *Experimental Biology and Medicine Journal* **23**, 81–90.

Poinapen, J. & Ekama, G. A. 2010 Biological sulphate reduction with primary sewage sludge in an upflow anaerobic sludge bed reactor – part 5: steady-state model. *Water SA* **36** (3), 193–202.

Roussel, J. & Carliell-Marquet, C. 2016 Significance of vivianite precipitation on the mobility of iron in anaerobically digested sludge. *Frontiers in Environmental Science* **4** (60), 1–12.

Solon, K., Flores-Alsina, X., Kazadi Mbamba, C., Ikumi, D., Volcke, E. I. P., Vaneeckhaute, C., Ekama, G., Vanrolleghem, P. A., Batstone, D. J., Gernaey, K. V. & Jeppsson, U. 2017 Plant-wide modelling of phosphorus transformations in wastewater treatment systems: impacts of control and operational strategies. *Water Research* **113**, 97–110. https://doi.org/10.1016/j.watres.2017.02.007.

Tichy, R., Janssen, A., Grotenhuis, J. T. C., Van Abswoude, R. & Lettinga, G. 1998 Oxidation of biologically-produced sulphur in a continuous mixed-suspension reactor. *Water Research* **32** (3), 701–710.

Utgikar, V. P., Harmon, S. M., Chaudhary, N., Tabak, H. H., Govind, R. & Haines, J. R. 2002 Inhibition of sulfate-reducing bacteria by metal sulfide formation in bioremediation of acid mine drainage. *Environ. Toxicol.* **17**, 40–48.

Varga, E., Hauduc, H., Barnard, J., Dunlap, P., Jimenez, J., Menniti, A., Schauer, P., Lopez-Vazquez, C. M., Gu, A. Z., Sperandio, M. & Takács, I. 2018 Recent advances in bio-P modelling – a new approach verified by full-scale observations. In: *6th IWA/WEF Water Resource Recovery Modelling Seminar*, 10–14 March 2018, *Lac Beauport, QC, Canada*.

WERF 2007 Minimization of odors and corrosion in collection systems phase1 – 04-CTS-1. WERF, Alexandria, VA, USA.